View Article Online
View Journal

Dalton Transactions

An international journal of inorganic chemistry

Accepted Manuscript

This article can be cited before page numbers have been issued, to do this please use: E. Kuchuk, K. Giffin, A. Welle, K. Den Dauw, A. Fernandez, M. Cordier, T. Roisnel, J. Carpentier and E. Kirillov, *Dalton Trans.*, 2026, DOI: 10.1039/D6DT00602G.

This is an Accepted Manuscript, which has been through the Royal Society of Chemistry peer review process and has been accepted for publication.

Accepted Manuscripts are published online shortly after acceptance, before technical editing, formatting and proof reading. Using this free service, authors can make their results available to the community, in citable form, before we publish the edited article. We will replace this Accepted Manuscript with the edited and formatted Advance Article as soon as it is available.

You can find more information about Accepted Manuscripts in the Information for Authors.

Please note that technical editing may introduce minor changes to the text and/or graphics, which may alter content. The journal's standard Terms & Conditions and the Ethical guidelines still apply. In no event shall the Royal Society of Chemistry be held responsible for any errors or omissions in this Accepted Manuscript or any consequences arising from the use of any information it contains.

ROYAL SOCIETY OF CHEMISTRY

rsc.li/dalton

Ph_2Si-Bridged Constrained-Geometry Complexes of Hafnium and Titanium for Copolymerization of Ethylene and 1-Octene: An Experimental and Computational Comparison

View Article Online
DOI: 10.1039/D6DT00602G

Ekaterina Kuchuk,[a] Kaitie A. Giffin,[c] Alexandre Welle,[c] Katty Den Dauw,[c] Alvaro Fernandez,[c] Marie Cordier,[b] Thierry Roisnel,[b] Jean-Francois Carpentier*,[a] and Evgueni Kirillov*,[a]

[a] Univ Rennes, CNRS, Institut des Sciences Chimiques de Rennes (ISCR), UMR 6226, F-35042 Rennes, France

[b] Centre de diffraction X, Univ Rennes, CNRS, ISCR, UMR 6226, F-35700 Rennes, France

[c] TotalEnergies OneTech Belgium, Zone Industrielle Feluy C, B-7181 Seneffe, Belgium

Correspondance to jean-francois.carpentier@univ-rennes.fr, evgueni.kirillov@univ-rennes.fr

Keywords: Constrained-geometry catalysts, fluorenyl ligands, hafnium, titanium, ethylene, α-olefins, copolymers, polyolefin elastomers, plastomers

ABSTRACT

A series of new constrained-geometry hafnium and titanium complexes, including {Me_2Si(2,7-tBu$_2$Flu)NtBu}$HfCl_2$ (**1-HfCl$_2$**), Ph_2Si(2,7-tBu$_2$Flu)NtBu}$HfCl_2$ (**2-HfCl$_2$**) and Ph_2Si(2,7-tBu$_2$Flu)NtBu}$TiCl_2$ (**2-TiCl$_2$**), was synthesized and fully characterized using solution NMR spectroscopy and X-ray crystallography. These complexes were subsequently evaluated in the copolymerization of ethylene with 1-octene ($[C8]_0$ = 0.48–1.88 M), revealing striking differences in catalytic performance and properties of the resulting polyolefin elastomers/plastomers (POE/POP). The hafnium complexes **1-HfCl$_2$** and **2-HfCl$_2$** exhibited low catalytic activity, yielding polymers with broad molecular weight distributions and only modest incorporation of 1-octene. In contrast, the titanium complex **2-TiCl$_2$** demonstrated significantly higher catalytic activity and achieved substantial 1-octene incorporation at an ethylene/1-octene molar ratio of ca. 6:1, with values reaching up to 36.6 mol%. **2-TiCl$_2$** exhibited approximately half the productivity of benchmark CGC {$Me_4CpSiMe_2N$*t*Bu}$TiCl_2$ (**3-TiCl$_2$**), yet yielding POE with a much higher molecular weight and a density of 0.8547 g·cm^{-3}. DFT calculations were also performed for the cationic catalytic species derived from the pre-catalysts **2-HfCl$_2$** and **2-TiCl$_2$** to rationalize the relative performance of the titled systems in incorporating ethylene and 1-octene and undergoing termination and transfer reactions. A +5.6 kcal·mol^{-1} energy difference (in terms of $\Delta\Delta H^{\neq}$) was computed between the transition states for the third ethylene insertion into the M−C(polymeryl) bond for the Hf-based system compared to the Ti-based system; other phenomena possibly plaguing efficiency of the Hf-system are discussed.

INTRODUCTION

Group 4 metal constrained-geometry catalysts (CGC)[1,2] remain one of the most extensively studied families of catalysts, known for their remarkable efficiency in producing ethylene/α-olefin (e.g. 1-octene) copolymers. These copolymers are of high industrial relevance for applications in coatings, car tires, polymer blends, foams, and impact modifiers used in polypropylene for automotive

View Article Online
DOI: 10.1039/D6DT00602G

components.[3] The versatility and efficiency of CGC systems, essentially those based on Ti and Hf, have made them indispensable in the production of such advanced materials with tailored properties. The molecular masses and comonomer incorporation levels of ethylene/1-octene copolymers synthesized with CGC systems are highly dependent on the structure of the (pre)catalyst. By modulating the ligand environment, CGC systems enable precise control over polymer properties, such as elasticity, toughness, low-temperature ductility, making them an essential tool in polymer chemistry. A landmark achievement in CGC technology is its successful commercialization by Dow through the INSITE™ technology, which revolutionized the production of specialty polyolefins. In line with its industrial success, academic interest in CGC systems persists due to the extensive structural diversity of potential catalyst designs and the opportunities for further optimization.[4]

The original CGC Ti system featuring a {$Me_4CpSiMe_2N$*t*Bu} ligand unit (Scheme 1, left)[5] demonstrates exceptionally high productivity in the copolymerization of ethylene and 1-octene, producing materials with high comonomer incorporation.[6,7] However, the resulting copolymers often exhibit relatively low molecular weights, which can limit their applicability in some contexts. Ongoing research has sought to address such challenges, exploring novel ligand frameworks and metal centers to enhance the performance of group 4 metal CGC systems.

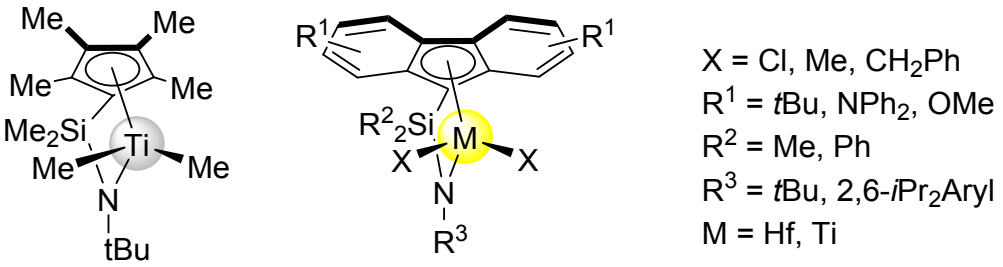

Scheme 1. Prototypical CGC titanium (left) and related {fluorenyl-amido} group 4 metal (right) (pre)catalysts.

View Article Online
DOI: 10.1039/D6DT00602G

Thus, the modification of CGC systems through the introduction of bulky substituted fluorenyl moieties (e.g., 2,7-*t*Bu_2-Flu, 3,6-*t*Bu_2-Flu, Oct = octamethyloctahydrofluorene)[8,9,10,11,12,13,14,15,16,17,18,19,20,21,22,23,24,25,26] or other structural modifications[27] in place of the Me_4Cp moiety, as well as varying substituents on the nitrogen atom, remains a widely explored strategy for fine-tuning the geometry and electronic properties, and in turn the catalyst's performance of CGC systems. As part of studies aimed at varying the nature of the metal center, fluorenyl-zirconium-based CGC systems have also been extensively investigated over the past decades, highlighting the specific role of steric expansion of the fluorenyl moiety in stabilizing the catalyst in its active form.[28,29,30,31,32]

In recent years, entirely new types of geometrically constrained titanium complexes have been synthesized, broadening the scope of CGC designs.[33] Numerous research groups have investigated these systems in various polymerization processes,essentially focusing on the homo- and co-polymerization of ethylene, e.g. ethylene/propylene, ethylene/1-octene, ethylene/norbornene,[8,9,10,13,16,17,18,19,23,24,25,26,34,35] but also polymerization of methyl methacrylate (MMA), 1,3-butadiene and styrene.[15,20,27,36,37]

In the present study, we investigated the catalytic potential of a series of new fluorenyl-based CGC complexes incorporating either Me_2Si- or the bulkier Ph_2Si- bridge (Scheme 1, right) for the copolymerization of ethylene with 1-octene. Given the distinct advantages of hafnium-based polymerization catalysts, which may exhibit greater thermal stability than their titanium (and zirconium) counterparts,[38,39] – a feature essential for high-temperature solution polymerization processes –, our approach was to synthesize and evaluate complexes of both metals. The dual focus on Ti and Hf CGC complexes aims at leveraging the individual strengths of these metals, with Ti systems potentially offering enhanced incorporation efficiency and Hf systems possibly providing a better thermal stability under demanding (co)polymerization conditions.

RESULTS AND DISCUSSION

The synthesis of the fluorenyl-amine proligands **1** and **2** was achieved by a regular two-step approach (Scheme 2).[40] The consistency of the products was confirmed by ^{1}H NMR spectroscopy (see the Supp. Info., Figures S1 and S2 for **b** and **2**, respectively). The proligands were then used for the synthesis of the corresponding hafnium (**1-HfCl$_2$**, **2-HfCl$_2$**) and titanium (**2-TiCl$_2$**) complexes, following a regular salt-metathesis approach. Hafnium complexes were isolated in 48% and 44% yields, respectively as light-yellow powders. **2-TiCl$_2$** was recovered after workup as a dark-violet solid in 77% yield, which after recrystallization afforded crystals in 6% yield. The consistency and purity of these complexes were confirmed by ^{1}H and ^{13}C NMR spectroscopy (Figures S3–S8, respectively), X-ray crystallographic studies and combustion analysis.

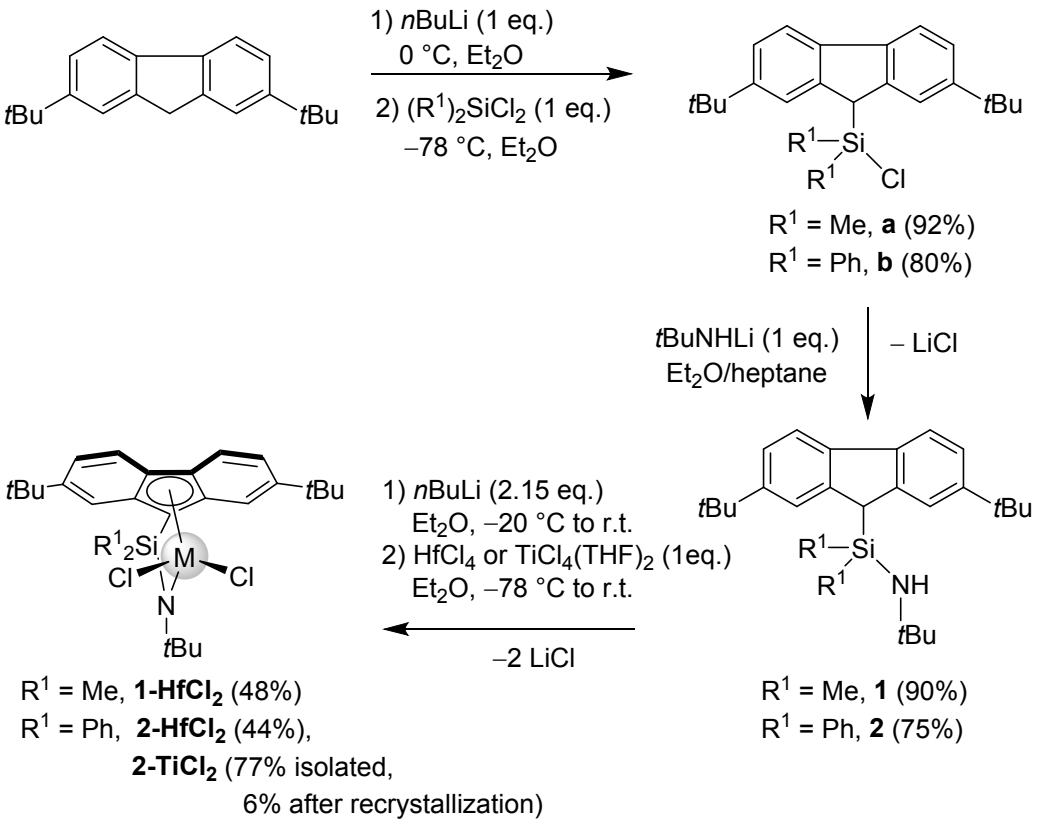

Scheme 2. Synthesis of proligands **1** and **2** and corresponding CGC complexes **1-HfCl$_2$, 2-HfCl$_2$** and **2-TiCl$_2$**.

View Article Online
DOI: 10.1039/D6DT00602G

The solid-state molecular structures of hafnium complexes **1-HfCl$_2$** and **2-HfCl$_2$** and titanium complex **2-TiCl$_2$** are shown in Figures S9, S10 and 1, respectively. Selected bond distances (Å) and angles (deg) are reported in Table 1. All the geometrical parameters, including bond lengths and angles, and overall coordination environment are comparable with those observed in analogous complexes, e.g. {Me$_2$Si(Oct)N*t*Bu}Hf(CH$_2$Ph)$_2$ (**I-Hf**)[29] and {Me$_2$Si(2,7-*t*Bu$_2$Flu)N(CMe$_2$Ph)}TiMe$_2$ (**II-Ti**),[23] respectively.

Table 1. Selected bond distances (Å) and angles (deg) for CGC complexes **1-HfCl$_2$**, **2-HfCl$_2$·(C$_6$H$_6$)** and **2-TiCl$_2$·(C$_6$H$_6$)** and reference complexes **I-Hf** and **II-Ti**.

	I-Hf [29]	**1-HfCl$_2$**	**2-HfCl$_2$·(C$_6$H$_6$)**	**II-Ti** [23]	**2-TiCl$_2$·(C$_6$H$_6$)**
M–Cl(1)	-	2.3645(8)	2.3656(6)	-	2.2688(5)
M–Cl(2)	-	2.3696(8)	2.3691(6)	-	2.2649(4)
M–N	2.087(8)	2.015(2)	2.0300(17)	1.922(12)	1.9093(12)
M–C(1)	2.373(11)	2.351(3)	2.343(2)	2.250(14)	2.210(14)
M–C(2)	2.550(10)	2.474(3)	2.516(2)	2.384(14)	2.433(14)
M–C(3)	2.685(11)	2.610(3)	2.619(2)	2.599(14)	2.595(15)
M–C(4)	2.697(13)	2.613(3)	2.587(2)	2.615(15)	2.558(14)
M–C(5)	2.500(13)	2.479(3)	2.426(2)	2.430(15)	2.334(14)
M–Flu$_{cent}$	2.251(10)	2.185(3)	2.177(2)	2.132(14)	2.098(14)
Flu$_{cent}$–M–N	105.87(5)	106.38(3)	105.16(2)	111.58(6)	110.52(6)
Cl(1)–M–Cl(2)	-	103.27(3)	103.89(2)	-	102.604(18)
N1–Si–C(1)	97.8(5)	93.97(11)	93.92(9)	94.20(6)	92.01(6)

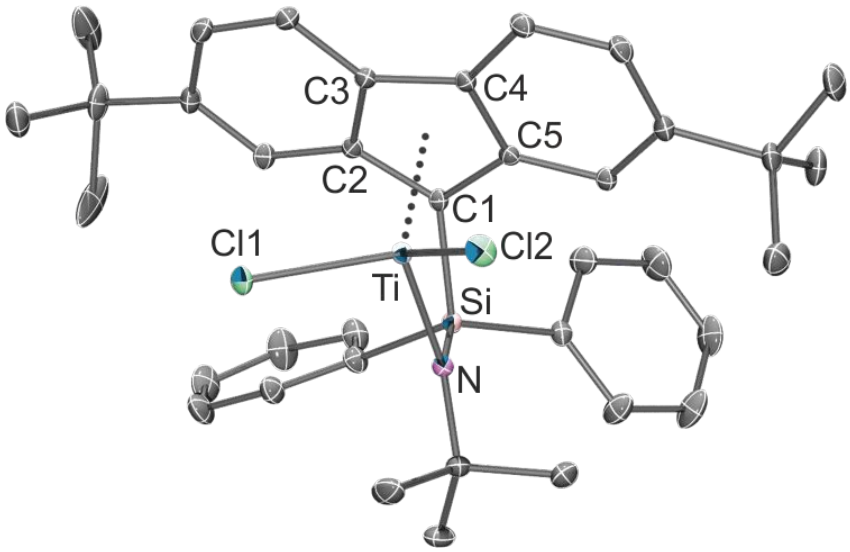

Figure 1. ORTEP representation of the solid-state molecular structure of **2-TiCl$_2$·(C$_6$H$_6$)** (H atoms omitted for clarity; ellipsoids drawn at the 50% probability level).

View Article Online
DOI: 10.1039/D6DT00602G

Polymerization studies. Copolymerization of ethylene and 1-octene was explored using the hafnium (**1-HfCl$_2$**, **2-HfCl$_2$**) and titanium (**2-TiCl$_2$**) complexes in combination with Al*i*Bu$_3$ (TIBAL) / [PhNMe$_2$H]$^+$[B(C$_6$F$_5$)$_4$]$^-$ as activator (cocatalyst). Although metallocene/borate cocatalyst systems are typically used with a 1:1 stoichiometric ratio, catalyst productivity in such dichlorometallocene/TIBAL/borate systems is known to increase with increasing borate concentration, up to a [B]/[M] molar ratio of 3:1.[41,42] Therefore, this ratio was systematically employed in this study. Representative results obtained from experiments carried out at 35 bar ethylene pressure in a 100 mL reactor magnetically stirred are reported in Table 2. The productivity observed for **1-HfCl$_2$** in homopolymerization of ethylene was low (entry 1; 135 kg$_{PE}$·mol$_{Hf}^{-1}$·h^{-1}), in contrast to **2-TiCl$_2$**, which afforded polyethylene (PE) with a productivity of 3,090 kg$_{PE}$·mol$_{Ti}^{-1}$·h^{-1} under similar conditions (entry 6).

In the copolymerization experiments ([C8]$_0$ = 0.48–1.88 M), the productivities observed for the hafnium complexes **1-HfCl$_2$** and **2-HfCl$_2$** were also quite low (131–141 kg$_{Pol}$·mol$_{Hf}^{-1}$·h^{-1}), regardless of the temperature employed (up to 130 °C) or the nature of the silylene bridge substituents (Me$_2$Si vs. Ph$_2$Si) (entries 2–5).* In striking contrast, the Ti analogue **2-TiCl$_2$** exhibited remarkably high productivities at 130 °C (8,030–23,780 kg$_{Pol}$·mol$_{Ti}^{-1}$·h^{-1}) over a range of catalyst

* The low productivity of the Hf systems may stem from instability or formation of Hf-Al bimetallic adducts (*vide infra*). Deleterious, excessive coordination of PhNMe$_2$ (released from the activator) to the active cationic hafnium species is likely to be discarded. Indeed, PhNMe$_2$ is usually considered as a poor base, very weakly or essentially non-coordinating to early transition metals. In fact, reports about the use of pyridylamido hafnium complexes for 1-hexene polymerization and ethylene/1-octene copolymerization (in the presence of Al(*n*-oct)$_3$; hence quite related to the present investigations) mention essentially identical productivity and polymer characteristics (in 1-hexene homopolymerization) upon activation with either [PhNMe$_2$H]$^+$[B(C$_6$F$_5$)$_4$]$^-$ or [Ph$_3$C]$^+$[B(C$_6$F$_5$)$_4$]$^-$ (see reference 35).

View Article Online
DOI: 10.1039/D6DT00602G

concentrations ([Ti]$_0$ = 2.6–11.2 μM; entries 7–10). In general, the productivity of this system in ethylene/1-octene copolymerization was higher than in ethylene homopolymerization, confirming that the so-called "comonomer effect" is operative for **2-TiCl$_2$**.[43]

Unexpectedly, the molecular weights (M_w) of the copolymers obtained with the Ti-based CGC system were significantly higher than those of the polymers obtained with the Hf ones (compare entries 3 and 7–10, respectively). In these cases, the broad polydispersities observed ($M_w/M_n = Đ_M$ in the range 3.8−22.2) could indicate apparent multi-site behavior of the catalytic systems under the polymerization conditions employed, with possible contributions from mass-transfer limitations arising from magnetic stirring in the 100 mL reactor (vide infra). In the case of systems based on the larger ionic radius Hf, the apparent multi-site behavior may additionally originate from catalyst decomposition on the timescale of a single chain-growth event, as well as from the formation of bimetallic species with R_3Al (where R = H, Me, *i*Bu or polymeryl), which may undergo disproportionation or evolve into other complex structures.[44,45]

The thermal transitions (melting, T_m, crystallization, T_c, and glass transition, T_g) determined for the copolymers obtained with **2-TiCl$_2$** were found within a narrow range of 2–3 °C, regardless the significant differences in the corresponding molecular weight (M_w = 366.0 and 629.7 kg·mol^{-1}) and incorporated 1-octene content (29.1 and 23.1 mol% at [C8]$_0$ = 1.83 M, respectively; compare entries 8 and 10). The observation of two crystallization transitions (T_c) for both samples may also be attributed to the multi-site nature of these polymerization reactions, which results in different crystallizable polymer fractions.

Two polymerization experiments conducted in a 1 L reactor equipped with mechanical stirring at 100 °C and 32 bar ethylene pressure, and at an ethylene/1-octene molar ratio of ca. 6:1 in the presence of H_2, showed similar trends in terms of overall productivity (Table 3). Under these conditions, **1-HfCl$_2$** proved completely inactive, whereas **2-TiCl$_2$** exhibited very high productivity (129,730 $kg_{Pol}·mol_{Ti}^{-1}·h^{-1}$). Improved control over the polymerization was achieved, as evidenced

View Article Online
DOI: 10.1039/D6DT00602G

by a much narrower polydispersity ($Đ_M$ = 2.3),† still affording a high molecular weight (M_w = 340.5 kg·mol^{-1}). The incorporated 1-octene content (20.1 mol% at $[C8]_0$ = 0.48 M) highlights the high propensity of this Ti CGC system to incorporate α-olefins (Figure S15). The corresponding polymer density (0.8547 g·cm^{-3}) is significantly lower than that of conventional PE (0.91–0.93 g·cm^{-3}) and falls in the lower limit of the range for typical POP/POE materials (0.86–0.90 g·cm^{-3}).[46]

For a direct comparison, the performance of the benchmark CGC {(Me_4Cp)$SiMe_2N$*t*Bu}$TiCl_2$ (**3-TiCl$_2$**) was evaluated under identical conditions (Table 3, entry 3). The reference catalyst appeared to be nearly twice as productive as **2-TiCl$_2$**, although it afforded a significantly (about one order of magnitude) lower molecular weight copolymer (M_w = 40.1 kg·mol^{-1}) and a higher density (0.8601 g·cm^{-3}).

^{13}C NMR analysis of both polymer samples produced by **2-TiCl$_2$** and **3-TiCl$_2$** (Table 3, entries 2 and 3) featured similar end-chains, with 29 and 27 saturated end-chains per 10,000 C, respectively, and no vinyl end-groups detected; this hints at very low β-H elimination (*vide infra*).

† The much narrower dispersity observed in this reactor equipped with efficient mechanical stirring may suggest that the aforementioned large polydispersities observed in the magnetically stirred reactor may actually be arising, at least in part, from mass transfer limitations; yet, a positive effect of H_2 addition as a regenerating and transfer agent is also clearly anticipated under these conditions.

Table 2. (Co)polymerization of ethylene and 1-octene (C8) with CGC systems **1-HfCl$_2$**, **2-HfCl$_2$** and **2-TiCl$_2$**.[a]

Entry	Precat	$[M]_0$ [μM]	Co-cat [B/M]	Temp [°C]	$[C8]_0$ [M]	m_{pol} [g]	Productivity [$kg_{pol}\cdot mol_{cat}^{-1}\cdot h^{-1}$]	T_g [b] [°C]	T_c [b] [°C]	T_m [b] [°C]	M_w [c] [$\times 10^3$] [$g\cdot mol^{-1}$]	M_w/M_n [c]	C_8 incorp [d] [mol%]
1	**1-HfCl$_2$**	12.1	3.0	130	0	0.042	135	n.a	119.8	137.3	n.a.	n.a.	0
2		12.0	3.0	100	1.83	0.044	141	n.o	111.5	124.4	n.a.	n.a.	n.a.
3		12.0	3.0	130	1.83	0.041	131	n.a	n.a	n.a	78.2	22.2	7.8
4	**2-HfCl$_2$**	11.6	3.1	60	1.83	0.031	103	–59.4	121.8	128.4/123.2/112.9	n.a.	n.a.	n.a.
5		11.4	3.2	100	1.83	0.033	112	–68.4	117.6/112.8	120.4/112.7	n.a.	n.a.	n.a.
6 [e]	**2-TiCl$_2$**	5.8	3.4	130	0	0.45	3,090	n.a	128.1	134.2	n.a.	n.a.	0
7 [f]		2.6	3.1	130	1.88	1.56	23,780	–66.7	95.8	115.8	496.1	3.8	36.6
8 [g]		5.6	3.4	130	1.84	2.21	15,160	−65.1	67.4/97.6	113.2	366.0	5.7	29.1
9		11.2	3.1	130	1.83	2.97	10,190	–67.3	100.0	114.5	305.4	4.3	29.6
10		11.2	3.2	130	1.83	2.34	8,030	−63.8	73.4/100.9	114.7	629.7	10.7	23.1

[a] General polymerization conditions unless otherwise stated: 100 mL-high pressure metallic reactor; solvent: isopar-G; ca. 50 mL of the liquid phase; 35 bar of ethylene; 15 mL (95.6 mmol) of 1-octene (1.83 M, 30% *v/v*); TIBAL = 0.30 mL neat (i.e., 1.20 mmol, [Al] = 24.0 mM); cocatalyst: $[PhNMe_2H]^+[B(C_6F_5)_4]^-$; reaction time = 30 min; n.a. = not analyzed, n.o. = not observed. [b] Determined by DSC from second run. [c] Determined by SEC in 1,2,4-trichlorobenzene at 135 °C vs. polystyrene standards (uncorrected values). [d] Determined by SEC equipped with a FTIR detector; [e] TIBAL = 0.71 mL of a 1M solution in toluene (i.e., 0.71 mmol, [Al] = 14.2 mM). [f] TIBAL = 0.32 mL of a 1M solution in toluene (0.32 mmol, [Al] = 6.4 mM). [g] TIBAL = 0.18 mL neat (0.71 mmol, [Al] = 14.2 mM).

Table 3. Copolymerization of ethylene and 1-octene (C8) with CGC systems **1-Hf-Cl$_2$** and **2-Ti-Cl$_2$** in the presence of H_2.[a]

entry	Precat	$[M]_0$ [μmol]	[B]/[M]	$[C8]_0$ [M]	m_{pol} [g]	Productivity [$kg_{pol}\cdot mol_{cat}^{-1}\cdot h^{-1}$]	T_g [b] [°C]	T_c [b] [°C]	T_m [b] [°C]	M_w [$\times 10^3$] [b] [$g\cdot mol^{-1}$]	M_w/M_n [b]	Density [c] [$g\cdot cm^{-3}$]	C8 incorp [d] [wt%]	C8 incorp [d] [mol%]
1	**1-HfCl$_2$**	0.74	3.0	0.48	0	0	n.a	n.a	n.a	-	-	-	-	-
2	**2-TiCl$_2$**	0.74	3.0	0.48	16.0	129,730	–55.1	n.o	n.o	340.5	2.3	0.8547	50.3	20.1
3	**3-TiCl$_2$**	0.76	3.0	0.48	36.2	285,650	–52.6	n.o	n.o.	40.1	2.4	0.8601	48.5	19.1

[a] General polymerization conditions otherwise stated: 1 L reactor; cocatalyst: $[PhNMe_2H]^+[B(C_6F_5)_4]^-$; solvent: *n*-hexane (425 mL); reaction time = 10 min; 2.0 mL TIBAL (10% *v/v* in hexane); P_{C2H4} = 32 bar; T_{pol} = 100 °C; H_2 = 800 ppm; n.a. = not analyzed, n.o. = not observed [b] Determined by SEC in 1,2,4-trichlorobenzene at 135 °C vs. polystyrene standards (uncorrected values). [c] Measured according to the ISO 1183-1:2012 standard method, method A at 23 °C. [d] Determined by ^{13}C NMR spectroscopy at 130 °C in C_6D_6/1,2,4-trichlorobenzene.

View Article Online
DOI: 10.1039/D6DT00602G

Theoretical calculations. In order to better rationalize the observed catalytic performance of the Hf- and Ti-based CGC systems, we conducted theoretical (DFT) computations using our previously developed theoretical model.[47,48]

The Hf and Ti CGC systems showed markedly different computed reactivity trends toward ethylene, within the intrinsic precision limits of the DFT method (Schemes S1, 3 and 4). For example, the first ethylene coordination/insertion into the cationic species [{Ph_2Si(2,7-$t$$Bu_2$Flu)N$t$Bu}M−Me]$^+$ (**A**, M = Hf or Ti), corresponding to the activation step (Scheme S1), displayed nearly identical reaction enthalpies ($\Delta_r H$ = 19.7–20.0 kcal·mol^{-1}) for both metals affording [{Ph_2Si(2,7-$t$$Bu_2$Flu)N$t$Bu}M−$n$-propyl]$^+$ (**C**). However, the process was kinetically more favorable for Ti by $\Delta\Delta H^{\neq}$ of 6.5 kcal·mol^{-1}.

Because the second and third ethylene insertion steps are representative of the overall catalytic performance, they were computed for the cationic complex [{Ph_2Si(2,7-$t$$Bu_2$Flu)N$t$Bu}M−$n$-propyl]$^+$ (**C**, where M = Hf or Ti). The insertion of 1-octene at the third step, following ethylene insertion, was also evaluated. The main results are summarized in Table 4 and illustrated in Schemes 3 and 4.

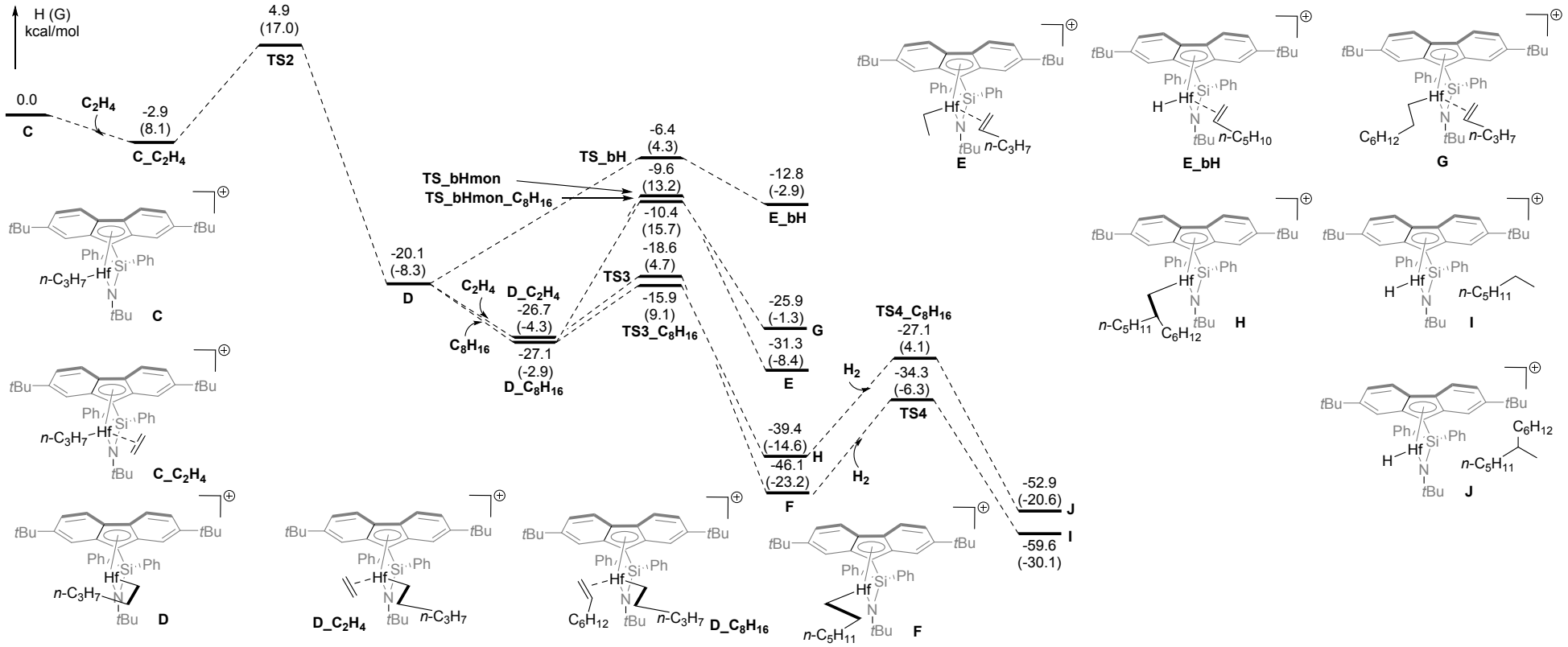

Scheme 3. Energy profile computed for ethylene/1-octene coordination/insertion, β-H elimination (BHE) and β-H transfer (BHT) steps for [{Ph_2Si(2,7-tBu$_2$Flu)NtBu}Hf–n-propyl]$^+$ (**C**) (energies in kcal.mol^{-1} relative to **C**).

View Article Online
DOI: 10.1039/D6DT00602G

The 5.6 kcal·mol^{-1} energy difference (in terms of $\Delta\Delta H^{\neq}$) between the transition states (TS) for the third ethylene insertion into the M−C(polymeryl) bond suggests approximately a 10^4-fold higher polymerization rate for the Ti-based system compared to the Hf-based system (assuming equal comonomer concentrations) at 298 K. This computed difference is in line with the significant differences observed in the productivities of the Hf- and Ti-based systems, emphasizing the very low (co)polymerization efficiency observed with the Hf-based catalysts based on **1,2-HfCl$_2$**. The insertion of 1-octene following ethylene was found to be only slightly more favorable on thermodynamic grounds ($\Delta\Delta_r H$ = 1.8 kcal·mol^{-1}) in the case of **2-TiCl$_2$**, while virtually no difference was observed from a kinetic standpoint ($\Delta\Delta H^{\neq}$ = 0.3 kcal·mol^{-1}).

The ability to induce chain-termination reactions was also evaluated (Table 4 and Schemes 3 and 4). Yet, both Hf and Ti CGC systems revealed comparable reluctance toward β-H elimination (BHE) and β-H transfer (BHT) to the monomer (both ethylene and 1-octene) from a kinetic perspective, as indicated by the relatively high barriers compared to those for regular ethylene or 1-octene insertion ($\Delta H^{\neq}$ = 12.4−13.7 and 11.4−20.9 vs. 2.5−7.8 or 10.9−11.2 kcal·mol^{-1}, respectively).

Since small amounts of hydrogen were introduced in several polymerization experiments (Table 3) to control the molecular weight of the copolymers, transfer-to-hydrogen was also evaluated computationally (Scheme S2). Transfer-to-hydrogen appeared to be kinetically more favorable ($\Delta\Delta H^{\neq}$ = 2.9−7.5 kcal·mol^{-1}) for **2-TiCl$_2$**, regardless of the nature of the monomer inserted in the previous step. For the **3-TiCl$_2$** reference system, which produces lower molecular weight copolymers in the presence of hydrogen, the experimental data are consistent with the very low computed barriers ($\Delta H^{\neq}$ = 0.1−0.2 kcal·mol^{-1}) and the favorable thermodynamics of this process ($\Delta_r H$ = −13.6−16.2 kcal·mol^{-1}).

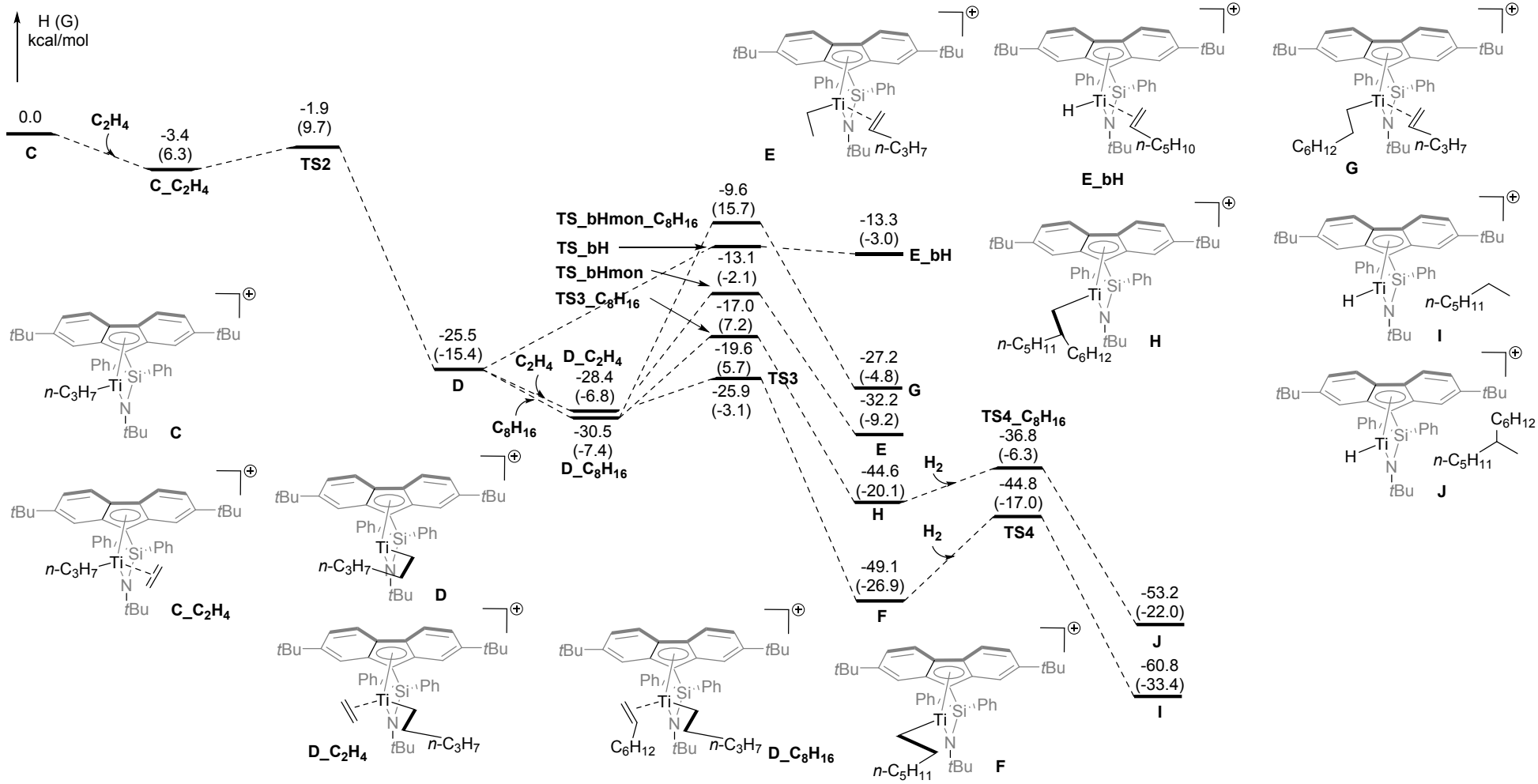

Scheme 4. Energy profile computed for ethylene/1-octene coordination/insertion, β-H elimination (BHE) and β-H transfer (BHT) steps for [{Ph_2Si(2,7-tBu$_2$Flu)NtBu}Ti−n-propyl]$^+$ (**C**) (energies in kcal.mol^{-1} relative to **C**).

View Article Online
DOI: 10.1039/D6DT00602G

Heterobimetallic ion pairs of the type $[\{LX\}_2M(\mu\text{–}R)AlR_2]^+[A]^-$ (where $\{LX\}_2M$ represents a group 4 metallocene-type core, R is an alkyl group, and $[A]^-$ denotes a counteranion such as ["MeMAO"]$^-$, $[B(C_6F_5)_4]^-$, etc.) are widely recognized as "dormant" species and precursors for chain transfer during olefin polymerization.[49,50] These species play a pivotal role in polymerization mechanisms, serving as intermediates that maintain the delicate balance between active and dormant states of the catalytic cycle.[51,52,53,54] Hence, we also computationally evaluated the thermochemistry associated with the formation of such heterobimetallic adducts derived from the insertion products, specifically the naked cations $[\{Ph_2Si(2,7\text{-}t\text{Bu}_2\text{Flu})N t\text{Bu}\}M\text{–}n\text{-pentyl}]^+$ (Scheme 5), with Al*i*Bu$_3$ (TIBAL, in its dimeric form $Al_2i\text{Bu}_6$),[55] employed in our study as co-activator and scavenger and, for comparison purposes, with $AlMe_3$ (TMA, in its dimeric form Al_2Me_6)[56] although it is not directly relevant to our catalysis. Consistent with previous reports on the strong binding affinity of cationic hafnocenes toward TMA,[57] our calculations (Table 4) also indicate a higher propensity of the Hf CGC system to reversibly coordinate TIBAL compared to its Ti analogue (and, expectedly, much more TMA than TIBAL). The coordination of TIBAL to the putative cationic alkyl active catalyst species does not appear to be favored; however, the low computed value (ΔH_{coord} = +0.9 kcal·mol^{-1}) for the Hf system suggests that it could represent a competitive deactivation pathway. This phenomenon, which results in blocking of the active site and prevents the coordination and insertion of olefin molecules, may also contribute to the significantly lower activity observed in the present Hf CGC systems. However, NMR investigations of mixtures of **1-Hf-Cl$_2$**/$[PhNMe_2H]^+[B(C_6F_5)_4]^-$/TIBAL yielded highly complex spectra that proved uninformative.

View Article Online
DOI: 10.1039/D6DT00602G

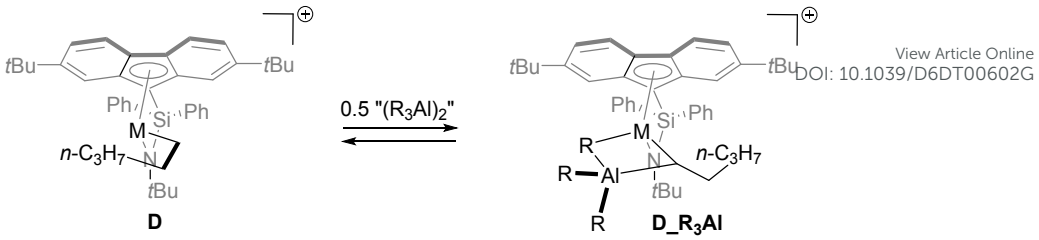

Scheme 5. Reversible formation of heterobimetallic cationic R_3Al-adducts from [{Ph_2Si(2,7-tBu$_2$Flu)NtBu}M−n-pentyl]$^+$ (where M = Hf, Ti) and R_3Al dimer (e.g. Al_2iBu_6 ≡ TIBAL dimer).

Table 4. Energetic data (kcal·mol^{-1}) calculated for ethylene coordination/insertion, β-H elimination (BHE) and β-H transfer (BHT) steps and TIBAL/TMA coordination with Hf and Ti CGC systems [{Ph_2Si(2,7-tBu$_2$-Flu)NtBu}M−R]$^+$.

		CGC system	
		Hf	**Ti**
2nd insertion	ΔH_{coord}	−2.9	−3.4
	$\Delta H^{\neq}$	7.8	5.3
	$\Delta_r H$	−20.1	−25.5
3d insertion (ethylene)	ΔH_{coord}	−6.6	−2.9
	$\Delta H^{\neq}$	8.1	2.5
	$\Delta_r H$	−19.4	−20.7
3d insertion (1-octene after ethylene)	ΔH_{coord}	−7.0	−5.0
	$\Delta H^{\neq}$	11.2	10.9
	$\Delta_r H$	−12.3	−14.1
BHE	$\Delta H^{\neq}$	13.7	12.4
	$\Delta_r H$	7.3	12.2
BHT (ethylene)	$\Delta H^{\neq}$	17.1	11.4
	$\Delta_r H$	−4.4	−3.8
BHT (1-octene)	$\Delta H^{\neq}$	16.7	20.9
	$\Delta_r H$	−1.2	−3.3
Transfer to H_2 (after ethylene insertion)	$\Delta H^{\neq}$	11.8	4.3
	$\Delta_r H$	−13.5	−11.7
Transfer to H_2 (after 1-octene insertion)	$\Delta H^{\neq}$	12.3	7.8
	$\Delta_r H$	−13.5	−8.6
Coordination of TIBAL (after ethylene insertion)	$\Delta_r H$	0.9	5.8
Coordination of TMA (after ethylene insertion)	$\Delta_r H$	−6.0	−2.5

CONCLUSIONS

Constrained-geometry dichloro complexes of hafnium and titanium from the {Flu/N}-family were synthesized and evaluated in the copolymerization of ethylene and 1-octene. These preliminary studies revealed that the Hf CGC complexes exhibit very low productivity; this may be attributed essentially to a more difficult insertion of the monomer (ethylene) into the Hf–C(polymeryl) bond as well as to the existence of concomitant deactivation pathways of the active cationic species involving alkylaluminum compounds. On the contrary, the Ti analogue **2-TiCl$_2$** exhibited significantly higher productivity in ethylene/1-octene copolymerization, featuring a clear "comonomer effect". The copolymers obtained with the Ti CGC system also displayed higher molecular weights; narrow polydispersity consistent with single site behavior of this Ti CGC system could be achieved in the presence of H_2 as reactivating/transfer agent in a mechanically stirred reactor. Thermal analysis revealed narrow ranges of melting, crystallization, and glass transition temperatures, with several crystallizable polymer fractions. Furthermore, the present Ti CGC system showed a high propensity to incorporate α-olefins, producing POE/POP-type materials with lower density. The cost-effectiveness of titanium compared to hafnium further enhances the appeal of **2-TiCl$_2$** as a promising candidate for large-scale production of POE/POP-type copolymers.

DATA AVAILABILITY

The data supporting this article have been included as part of the supplementary information (SI). Supplementary information: Fig. S1–S15, Scheme S1 and Tables S1 and S2; crystallographic data for CCDC **1-HfCl$_2$**, **2-HfCl$_2$** and **2-TiCl$_2$** (CCDC 2497781–2497783). See DOI: https://doi.org/

AUTHOR INFORMATION

Ekaterina Kuchuk, Univ Rennes, CNRS, ISCR UMR 6226, F-35042 Rennes, France

Kaitie A. Giffin, TotalEnergies OneTech Belgium, Zone Industrielle Feluy C, B-7181 Seneffe, Belgium

Alexandre Welle, TotalEnergies OneTech Belgium, Zone Industrielle Feluy C, B-7181 Seneffe, Belgium

Katty Den Dauw, TotalEnergies OneTech Belgium, Zone Industrielle Feluy C, B-7181 Seneffe, Belgium

Alvaro Fernandez, TotalEnergies OneTech Belgium, Zone Industrielle Feluy C, B-7181 Seneffe, Belgium

Thierry Roisnel, Univ Rennes, CNRS, Centre de diffraction X, ISCR UMR 6226, F-35042 Rennes, France

Marie Cordier, Univ Rennes, CNRS, Centre de diffraction X, ISCR UMR 6226, F-35042 Rennes, France

View Article Online
DOI: 10.1039/D6DT00602G

Corresponding Authors

Jean-François Carpentier*, Univ Rennes, CNRS, ISCR UMR 6226, F-35042 Rennes, France, E-mail: jean-francois.carpentier@univ-rennes.fr, ORCID: 0000-0002-9160-7662.

Evgueni Kirillov*, Univ Rennes, CNRS, ISCR UMR 6226, F-35042 Rennes, France, E-mail: evgueni.kirillov@univ-rennes.fr, ORCID: 0000-0002-5067-480X.

Author Contributions

The manuscript was written through contributions of all authors. All authors have given approval to the final version of the manuscript.

Notes

The authors declare no competing financial interest.

View Article Online
DOI: 10.1039/D6DT00602G

ACKNOWLEDGMENTS

This work was financially supported by TotalEnergies OneTech Belgium (postdoctoral fellowship to EAK). The authors are grateful to Jerome Ollivier for technical assistance in DSC analysis. EK gratefully acknowledges the *Institut Universitaire de France* (IUF) for a Senior IUF fellowship, and thanks ENSCR and the CTI group of ISCR for computational facilities.

REFERENCES

1 McKnight, A. L.; Waymouth, R. M. Group 4 *ansa* cyclopentadienyl-amido catalysts for olefin polymerization. *Chem. Rev.* **1998**, *98,* 2587–2598.

2 Braunschweig, H.; Breitling, F. M. Constrained Geometry Complexes – Synthesis and Applications. *Coord. Chem. Rev.* **2006**, *250*, 2691–2720.

3 Li, F.; Liu, W. Progress in the catalyst for ethylene/α-olefin copolymerization at high temperature. *Can. J. Chem. Eng.* **2023**, *101*, 4992–5019.

4 Chum, P. S.; Swogger, K. W. Olefin polymer technologies - History and recent progress at The Dow Chemical Company. *Prog. Polym. Sci.* **2008**, *33*, 797–819.

5 Okuda, J. Functionalized Cyclopentadienyl Ligands, IV. Synthesis and Complexation of Linked Cyclopentadienyl-Amido Ligands. *Chem. Ber.*, **1990**, *123*, 1649–1651.

6 Klosin, J.; Fontaine, P. P.; Figueroa, R. Development of Group IV molecular catalysts for high temperature ethylene-α-olefin copolymerization reactions. *Acc. Chem. Res.* **2015**, *48*, 2004–2016.

7 Bremer, S; Bellair, R.J.; Scholtz T. W.; Senecal, T. D.; Klozin J. Synthesis and evaluation of trialkyl ammonium tetrakis(pentafluorophenyl) aluminate, a highly efficient activator for high-temperature ethylene-α-olefin copolymerization reactions. *Organometallics* **2024**, *43*, 2651–2661.

8 Razavi, A.; Thewalt, U. Preparation and crystal structures of the complexes (η^5-C_5H_3 TMSCMe$_2$ η^5-$C_{13}H_8$)MCl_2 and [3,6-di-*t*Bu-$C_{13}H_6SiMe_2N$*t*Bu]MCl_2 (M=Hf, Zr or Ti):

mechanistic aspects of the catalytic formation of a isotactic-syndiotactic stereoblock-type polypropylene. *J. Organomet. Chem.* **2001**, *621*, 267–276.

9 Nishii, K.; Hagihara, H.; Ikeda, T.; Akita, M.; Shiono, T. Stereospecific polymerization of propylene with group 4 *ansa*-fluorenylamidodimethyl complexes. *J. Organomet. Chem*. **2006**, 691, 193–201.

10 Tanaka R.; Yanase, C.; Cai, Z.; Nakayama, Y.; Shiono, T. Structure-stereospecificity relationships of propylene polymerization using substituted *ansa*-silylene (fluorenyl)amido titanium complexes. *J. Organomet. Chem.* **2016**, *804*, 95–100.

11 Dias, H. V. R.; Wang, Z. Syntheses and characterization of zirconium and hafnium complexes of amido-fluorenyl ligands $[(NBu^t)SiMe_2CH_2(C_{13}H_8)]^{2-}$ and $[(NPr^i)SiMe_2CH_2(C_{13}H_8)]^{2-}$. *J. Organomet. Chem.* **1997**, *539,* 77–85.

12 Wang, W.; Qu, S.; Li, X.; Chen, J; Guo, Z; Sun, W.-H. Transition metal complex catalysts promoting copolymers of cycloolefin with propylene/higher olefins. *Coord. Chem. Rev.* **2023**, *494*, 215351.

13 Yuan, H.; Kida, T.; Tanaka, R.; Cai, Z.; Nakayama, Y.; Kihara, S., Shiono, T. Star polymers with norbornene/1-octene gradient copolymer arms synthesized by an *ansa*-fluorenylamidodimethyltitanium-$[Ph_3C][B(C_6F_5)_4]$ catalyst system. *Polymer* **2022**, *249*, 124844.

14 Alt, H. G.; Reb, A. Amido functionalized *ansa*-fluorenylidene half-sandwich complexes of zirconium as catalyst precursors for homogeneous ethylene polymerization. *J. Mol. Catal. A: Chem.* **2001**, *175*, 43–50.

15 Tanaka, R.; Nakayama, Y.; Shiono, T. Synthesis of high-molecular weight block copolymers of norbornene and propylene with methyl methacrylate initiated by a fluorenylamido titanium complex. *Polym. Chem.* **2013**, *4*, 3974.

16 Cai, Z.; Ikeda, T.; Akita, M; Shiono T. Substituent effects of *tert*-butyl groups on fluorenyl ligand in syndiospecific living polymerization of propylene with *ansa*-fluorenylamidodimethyl-titanium complex. *Macromolecules* **2005**, *38*, 8135–8139.

17 Cai, Z.; Harada, R.; Nakayama, Y.; Shiono, T. Highly active living random copolymerization of norbornene and 1-alkene with *ansa*-fluorenylamidodimethyl-titanium derivative: Substituent effects on fluorenyl ligand. *Macromolecules* **2010**, *43*, 4527–4531.

18 Hasan, T.; Ikeda, T.; Shiono, T. Random copolymerization of propene and norbornene with *ansa*-fluorenylamidodimethyl-titanium-based catalysts. *Macromolecules* **2005**, *38*, 1071–1074.

19 Sun, Y; Wang, C.; Tanaka, R.; Shiono, T.; Cai, Z. Copolymerization of ethylene and fluoroalkylnorbornene using highly active *ansa*-(fluorenyl)(amido)titanium-based catalysts. *Macromol. Chem. Phys.* **2019**, *220*, 1900306.

20 Song, X.; Ma, Q., Cai, Z., Tanaka, R., Shiono T.; Grubbs, R. B. Facile synthesis of novel polyethylene-based A-B-C block copolymers containing poly(methyl methacrylate) using a living polymerization system. *Macromol. Rapid Commun.* **2016**, *37*, 227−231.

21 Okuda, J.; Schattenmann, F. J.; Wocadlo, S.; Massa, W. Synthesis and characterization of zirconium complexes containing a linked amido-fluorenyl ligand. *Organometallics*, **1995**, *14*, 789–795.

22 Rajesh, A.; Sivaram, S. Polymerization of ethylene using amido functional half-sandwich complexes of group 4 metals. *Polym. Engin. Sci.* **2011**, *51*, 2103–2108.

23 Wang, H.; Wang H.; Sun, Y.; Cheng, H; Shiono, T.; Cai, Z. Living polymerization of propylene with *ansa*-dimethylsilylene(fluorenyl)(cumylamido) titanium complexes. *Polymers* **2017**, *9*, 131.

24 Wang, H.; Li, Y., Cai, Z. Substituent effects of phenyl group on silylene bridge in stereospecific polymerization of propylene with C_1-symmetric *ansa*-silylene(fluorenyl)(amido) dimethyl titanium complexes. *Polymers* **2018**, *10*, 1075.

25 Sun, Y.; Xu, B., Shiono, T.; Cai, Z. Highly active *ansa*-(fluorenyl)(amido)titanium-based catalysts with low load of methylaluminoxane for syndiotactic-specific living polymerization of propylene. *Organometallics* **2017**, *36*, 3009−3012.

26 Yuan, H.; Kida, T.; Kim, H.; Tanaka, R.; Cai, Z.; Nakayama, Y.; Shiono, T. Synthesis and properties of gradient copolymers composed of norbornene and higher α-olefins using an *ansa*-fluorenylamidodimethyl-titanium-$[Ph_3C][B(C_6F_5)_4]$ catalyst system. *Macromolecules* **2020**, *53*, 4323−4329.

27 Toda, T.; Miura, I.; Ohta, S.; Takenaka, K. Synthesis, structural analysis, and polymerization activity of noncyclopentadienyl constrained geometry complex $[Me_2Si(Ph_2C)(^tBuN)]ZrCl_2(thf)$. *Appl. Organomet. Chem.* **2024**, *38*, e7710.

28 Irwin, L. J.; Reibenspies, J. H.; Miller, S. A. A sterically expanded "Constrained Geometry Catalyst" for highly active olefin polymerization and copolymerization: An unyielding comonomer effect. *J. Am. Chem. Soc.* **2004**, *126*, 16716–16717.

29 Irwin, L. J.; Reibenspies, J. H.; Miller, S. A. Synthesis and characterization of sterically expanded *ansa*-η^1-fluorenyl-amido complexes. *Polyhedron* **2005**, *24*, 1314–1324.

30 Schwerdtfeger, E. D.; Miller, S. A. Intrinsic branching effects in syndiotactic copolymers of propylene and higher α-olefins. *Macromolecules* **2007**, *40*, 5662–5668.

31 Schwerdtfeger, E. D.; Irwin, L. J.; Miller, S. A. Highly branched polyethylene from ethylene alone via a single zirconium-based catalyst. *Macromolecules* **2008**, *41*, 1080–1085.

32 Chai, J.; Abboud, K. A.; Miller, S. A. Sterically expanded CGC catalysts: Substituent effects on ethylene and α-olefin polymerization. *Dalton Trans.* **2013**, *42*, 9139–9147.

33 Bao J; Li Y; Chan, C.-M.; Law, K.-C.; Yiu, S.-M.; Chan, M. C. W. Geometrically constrained cofacial bi-titanium olefin polymerization catalysts: Tuning and enhancing comonomer incorporation density. *ACS Catal*. **2024**, *14*, 17911−17918.

34 Shiono T. Living polymerization of olefins with *ansa*-dimethylsilylene(fluorenyl)(amido) dimethyl-titanium-based catalysts. *Polym. J.* **2011**, *43*, 331–351.

35 Kulyabin, P. S.; Uborsky, D. V.; Voskoboynikov, A. Z.; Canich, J. A. M.; Hagadorn, J. R. Pyridylamido hafnium complexes with a silylene bridge: synthesis and olefin polymerization. *Dalton Trans.* **2020**, *49*, 6693–6702.

36 Kaminsky, W; Hinrichs, B., Rehder, D. Diolefin polymerization by half-sandwich complexes and MAO as cocatalyst. *Polymer* **2002**, 7225−7229.

37 Kirillov, E; Razavi, A., Carpentier, J.-F. Syndiotactic-enriched propylene–styrene copolymers using fluorenyl-based half-titanocene catalysts. *J. Mol. Catal. A: Chem.,* **2006**, 230−235.

38 Li, F.; Liu, W. Progress in the catalyst for ethylene/α-olefin copolymerization at high temperature. *Can. J. Chem. Ing.* **2023**, *101*, 4992–5019.

39 Vittoria, A.; Goryunov, G. P.; Izmer, V. V.; Kononovich, D. S.; Samsonov, O. V.; Zaccaria, F.; Urciuoli, G.; Budzelaar, P. H. M.; Busico, V.; Voskoboynikov, A. Z.; Uborsky, D. V.; Ehm, C.; Cipullo, R. Hafnium vs. zirconium, the perpetual battle for supremacy in catalytic olefin polymerization: A simple matter of electrophilicity? *Polymers* **2021**, *13*, 2621.

40 Cai, Z.; Ikeda, T.; Akita, M.; Shiono, T. Substituent effects of *tert*-butyl groups on fluorenyl ligand in syndiospecific living polymerization of propylene with *ansa*-fluorenylamidodimethyl-titanium complex. *Macromolecules* **2005**, *38*, 8135–8139.

41 Song, F.; Cannon, R. D.; Lancaster, S. J.; Bochmann, M. Activator effects in metallocene-based alkene polymerisations:unexpectedly strong dependence of catalyst activity on tritylconcentration. *J. Mol. Catal. A: Chem.* **2004**, *218*, 21−28.

42 Ehm, C.; Mingione, A.; Vittoria, A.; Zaccaria, F.; Cipullo, R.; Busico, V. High-Throughput Experimentation in Olefin Polymerization Catalysis: Facing the Challenges of Miniaturization. *Ind. Eng. Chem. Res.* **2020**, *59*, 13940−13947.

43 Cruz, V. L.; Muños-Escalona, A.; Martinez-Salazar, J. A theoretical study of the comonomer effect in the ethylene polymerization with zirconocene castalytic systems. *J. Polym.Sci, A, Polym. Chem.* **1998**, *36*, 1157−1167.

44 Gotz, C.; Rau, A.; Luft, G. Ternary metallocene catalyst systems based on metallocene dichlorides and $AlBu^{i}_{3}$/$[PhNMe_2H][B(C_6F_5)_4]$. NMR investigations of the influence of Al/Zr ratios on alkylation and on formation of the precursor of the active metallocene species. *J. Mol. Cat. A: Chem.* **2002**, *184*, 95−110.

45 Baldwin, S. M.; Bercaw, J. E.; Henling, L. M.; Day, M. W.; Brintzinger, H. H.Cationic Alkylaluminum-Complexed Zirconocene Hydrides: NMR-Spectroscopic Identification, Crystallographic Structure Determination, and Interconversion with Other Zirconocene Cations. *J. Am. Chem. Soc.* **2011**, *133*, 1805−1813 and references cited therein.

46 Knuuttila, H.; Lehtinen, A.; Nummila-Pakarinen, A. Advanced polyethylene technologies - Controlled material properties. *Adv. Polym. Sci.* **2004**, *169*, 13–27.

47 Castro, L.; Kirillov, E.; Miserque, O.; Welle, A.; Haspeslagh, L.; Carpentier, J.-F.; Maron, L. Are solvent and dispersion effects crucial in olefin polymerization DFT calculations? Some insights from propylene coordination and insertion reactions with group 3 and 4 metallocenes. *ACS Catal.* **2015**, *5*, 416–425.

48 Castro, L.; Theurkauff, G.; Vantomme, A.; Welle, A.; Haspeslagh, L.; Brusson, J.-M.; Maron, L.; Carpentier, J.-F.; Kirillov, E. A. Theoretical outlook on the stereoselectivity origins of isoselective zirconocene propylene polymerization Catalysts. *Chem. Eur. J.* **2018**, *24*, 10784–10792.

49 Bochmann, M. The chemistry of catalyst activation: the case of group 4 polymerization catalysts. *Organometallics* **2010**, *29*, 4711–4740.

50 Chen, E. Y.-X.; Marks, T. J. Cocatalysts for metal-catalyzed olefin polymerization: activators, activation processes, and structure-activity relationships. *Chem. Rev.* **2000**, *100*, 1391–1434.

51 Theurkauff, G.; Bondon, A.; Dorcet, V.; Carpentier, J.-F.; Kirillov, E. Heterobi- and -trimetallic ion pairs of zirconocene-based isoselective olefin polymerization catalysts with $AlMe_3$. *Angew. Chem. Int. Ed.* **2015**, *54*, 6343−6346.

52 Theurkauff, G.; Bader, M.; Marquet, N.; Bondon, A.; Roisnel, T.; Guegan, J.-P.; Amar, A.; Boucekkine, A.; Carpentier, J.-F.; Kirillov, E. Discrete ionic complexes of highly isoselective zirconocenes. Solution dynamics, trimethylaluminum adducts, and implications in propylene polymerization. *Organometallics* **2016**, *35*, 258−276.

53 Desert, X.; Proutiere, P.; Welle, A.; Den Dauw, K.; Vantomme, A.; Miserque, O.; Brusson, J.-M.; Carpentier, J.-F.; Kirillov, E. Zirconocene-catalyzed polymerization of α-olefins: When intrinsic higher activity is flawed by rapid deactivation. *Organometallics* **2019**, *38*, 2664−2673.

54 Desert, X.; Carpentier, J.-F.; Kirillov, E. Quantification of active sites in single-site group 4 metal olefin polymerization catalysis. *Coord. Chem. Rev.* **2019**, *386*, 50−68.

55 Hermann, A.; Münch, A.; Orr, S. A.; Herbst-Irmer, R.; Mulvey, R. E.; Strohmann, C.; Stalke, D. When electrons step in: Polarizing effects explored with triisobutylaluminum. *Inorg. Chem.* **2021**, *60*, 2872−2877.

56 Vranka, R. G.; Amma, E. L. Crystal structure of trimethylaluminum. *J. Am. Chem. Soc.* **1967**, *89*, 3121−3126.

57 Busico, V.; Cipullo, R.; Pellecchia, R.; Talarico, G.; Razavi, A. Hafnocenes and MAO: Beware of trimethylaluminum! *Macromolecules* **2009**, *42*, 1789−1791.

View Article Online
DOI: 10.1039/D6DT00602G

DATA AVAILABILITY

The data supporting this article have been included as part of the supplementary information (SI). Supplementary information: Fig. S1–S15, Scheme S1 and Tables S1 and S2; crystallographic data for CCDC **1-$HfCl_2$**, **2-$HfCl_2$** and **2-$TiCl_2$** (CCDC 2497781–2497783). See DOI: https://doi.org/